View metadata, citation and similar papers at core.ac.uk
brought to you by CORE
provided by Open Archive Toulouse Archive Ouverte

Electrochimica Acta 52 (2007) 2580–2587

Classic and local analysis of corrosion behaviour of graphite and stainless steels in polluted phosphoric acid

H. Iken [a,*], R. Basseguy [b], A. Guenbour [a], A. Ben Bachir [a]

[a] *Laboratoire d'Electrochimie-Corrosion, Faculté des Sciences, Université Mohamed V, Av. Ibn Batouta, BP 1014 Rabat, Morocco*
[b] *Laboratoire de Génie Chimique UMR-CNRS 5503 Basso Cambo, 5 rue Paulin Talabot, BP 1301, 31106 Toulouse, France*

Received 25 April 2006; received in revised form 24 August 2006; accepted 6 September 2006
Available online 27 October 2006

Abstract

In phosphoric acid solution (40% H_3PO_4), the corrosion behaviour of graphite and stainless steels was studied by the use of different electrochemical methods, namely polarization curve analysis, electrochemical impedance spectroscopy (EIS) and scanning vibrating electrode technique (SVET). The combined effect of chemical impurities and the increase of medium temperature was studied to approach the real conditions in the process of phosphoric acid manufacturing. It was found that the current density measured by polarization curves increased with the presence of chloride and sulphate ions in the acid solution whatever the tested material. Compared to stainless steels, graphite had the best corrosion resistance in polluted phosphoric acid. However, for graphite the increase of temperature from 20 to 80 °C induced an increase of the corrosion rate and potential and a decrease of the resistance confirmed by EIS results. Subsequently, local currents were detected at the surface of the sample by using the scanning vibrating electrode technique. From the data obtained, graphite surface manifested a distinctive behaviour from that of stainless steels. A generalized corrosion was occurred on graphite whereas a localized corrosion was observed for stainless steels. These results show a clear interest of graphite as component material in some of the equipments of the phosphoric acid industry.
© 2006 Elsevier Ltd. All rights reserved.

Keywords: Corrosion; Graphite; Alloys; Phosphoric acid; Scanning vibrating electrode technique

1. Introduction

In the phosphoric acid industry, the main stages of the wet process phosphoric acid (WPA) manufacture involve the attack of phosphate ore by concentrated sulphuric acid (98%), filtration of the pulp and concentration of acid. This process generates severe corrosion problems of the equipments made of stainless steels and graphite (heat exchangers) due to the aggressiveness of the acid produced [1].

In our laboratory, several works studied the corrosion of various materials in the phosphoric acid with addition of chemical ions [2–5] and solid particles (abrasion effect) [6] and sometimes measurements were performed in the industrial phosphoric acid to study the behaviour in a real but complex medium [7]. All these studies were realized by using classic electrochemical techniques (voltametry, chronopotentiometry), spectroscopic and microscopic observations.

Stainless steels proved their good corrosion resistance in acid solutions. It was shown that chloride and sulfide ions accelerated the anodic process by altering passivity and activating the material dissolution rate. This harmfull effect was attributed to the adsorption of ions on the material surface [8–16].

Carbon materials are also very attractive for industrial applications [17,18] due to their chemical and electrochemical characteristics [19]. The corrosion of carbon was studied by many authors [20–28]. Kinoshita and Bett [20,21] reported that the formation of a surface oxide and evolution of carbon dioxide (CO_2) occurred during the electrochemical oxidation of different carbons in H_3PO_4 solution at temperatures up to 135 °C. A protective oxide (graphite oxide) and a surface oxide were found to form when the anodic current was imposed during the electrolysis of carbon electrodes in HCl [22].

Classic electrochemical techniques provide average data (corrosion potential, corrosion current, ...) integrating over a large surface area of the studied material. However, corrosion

* Corresponding author. Tel.: +212 37 77 54 40; fax: +212 37 77 54 40.
E-mail addresses: hichamiken@yahoo.fr (H. Iken), guenbour@fsr.ac.ma (A. Guenbour).

0013-4686/$ – see front matter © 2006 Elsevier Ltd. All rights reserved.
doi:10.1016/j.electacta.2006.09.013

phenomena are often localized, from where the interest of using local electrochemical analysis.

The scanning vibrating electrode technique (SVET) appears as powerful electrochemical technique to study oxido-reduction reactions in the micro range [29]. This technique is used in situ to measure the current densities on the corroded surface, without altering the corrosion process, nor to change the local environment in the localized corrosion sites, and without influencing the corrosion rate. SVET offer the possibility of mapping variations in current densities at the microscale over metal surface by measuring potential gradients developed in the solution due to the ionic flow. The maps show the spatial distribution of anodic and cathodic zones over a corroding surface and permits to evaluate the area ratio responsible of a global behaviour.

The SVET found a wide range of applications in the study of corrosion phenomena [30–33]; this technique uses a mobile microelectrode to detect and quantify localised corrosion currents occurring at the metal–electrolyte interface as pitting and crevice corrosion, surface microcracks, weld corrosion, galvanic and intergranular corrosion, corrosion in coated steel samples and deterioration of organic coatings.

The purpose of the present paper is to report on use of the classic and local electrochemical techniques for studying corrosion behaviour of graphite and stainless steels in a phosphoric acid solution and for investigating the influence of the medium temperature (20–80 °C) and the presence of pollutions (Cl^-, SO_4^{2-}). The addition of chloride and sulphate ions was used to mimic the chemical composition of the industrial phosphoric acid and the temperature was increased to 80 °C to approach the conditions at the concentration stage in the manufacturing process. The scanning vibrating electrode technique was specially used to detect the anodic and cathodic current distribution on the surface of the electrodes and then to determine the corrosion type.

2. Experimental

The materials used in this investigation are graphite impregnated with a fenolic resin and stainless steels Hastelloy G (HG), Uranus B64 (UB64) and Uranus 50 (U50). The chemical composition of the alloys is listed in Table 1. For all measurements, electrodes were mechanically polished using successively thinner grade of emery papers (400–4000 grades), then washed with distilled water and dried with blowing warm air. The exposed area of the specimen was 0.25 cm^2. Platinum and saturated calomel electrodes (sce) were used as counter and reference electrodes, respectively. The electrolyte used in this study was the phosphoric acid (40% H_3PO_4) without or with addition of 4% of H_2SO_4 and 400 ppm of chloride ions. In this last case, the solution was called polluted H_3PO_4 solution.

Anodic polarization curves were drawn potentiodynamically at a scan rate of 0.5 mV/s with a potentiostat/galvanostat EG&G model 263A. A cathodic potential at −0.3 V under the corrosion potential was imposed during 15 min before scanning potential towards anodic values.

A solartron SI 1250 frequency response analyser was used for electrochemical impedance spectroscopy (EIS). EIS diagrams were recorded between 20 and 10 mHz at the open-circuit potential and the ac amplitude was 10 mV. Before impedance test, the specimens were immersed in the electrolyte for 20 min to allow dynamic stabilization.

Local current measurements were performed using the SVET from Applicable Electronics (USA). Pt–Ir microelectrodes (Micro Probe Inc., USA) were black platinised before being used as probe. The diameter of the sphere of the black platinum deposit was about 20 μm with a corresponding capacitance of around 40 nF. The amplitude of the vibration used was about 20 μm and the vibration frequencies were between 200 and 300 Hz according to *X* and *Z* directions. The ASET Software (Science Wares Inc., USA) converted the potential drop measured by the microprobe with Ohm's law into a current density value. The calibration was made thanks to a stainless steel microelectrode used as a punctual current source. The displacement of the microprobe was performed using a motorised and computer controlled XYZ micromanipulator. A video camera was used to image and control the distance between the microprobe and the sample surface. This distance was 100 μm and the electrolyte used for all the SVET investigations was dilute chloridric acid solution (1 mM, pH 2.56 and conductivity 9.5 mS/cm). The local analysis was performed at open potential and at room temperature. Before SVET scans, graphite and stainless steel samples were immersed 60 min at open-circuit potential in polluted H_3PO_4 solution at different temperatures and washed with distilled water. Three treatments were carried out for each electrode, and three measurements were taken at various places of each analysed surface. The data were then treated with Matlab software and the current density was plotted as a three-dimensional surface (the current density measured along the *z*-axis as a function of the *x*, *y* plane). In this format, positive and negative current densities represent anodic and cathodic sites, respectively.

3. Results and discussion

3.1. Behaviour in H_3PO_4 solution at 20 °C

The polarization curves obtained on graphite and stainless steels in phosphoric acid solution (40% H_3PO_4 at 20 °C) are illustrated in Fig. 1.

Table 1
Chemical composition (wt%) of stainless steels

Alloy	Ni	Cr	Mo	Cu	Mn	Si	C	Other
HG	45.3	21.87	6.35	1.79	1.35	0.34	0.02	Ta: 2.43
UB64	25.56	20.58	4.67	2.36	1.24	0.72	0.017	W: 4
U50	8	21	2.5	1.5	2	1	0.03	N: 0.15

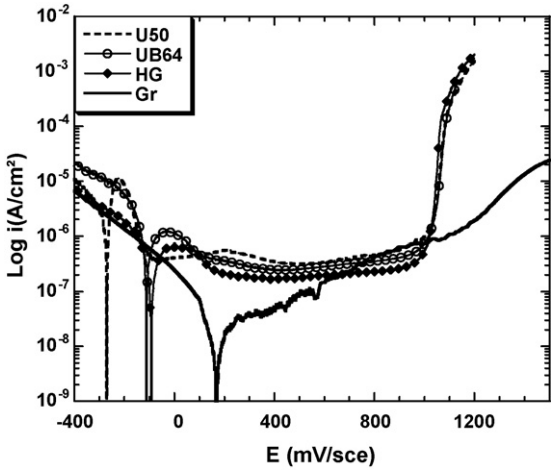

Fig. 1. Potentiodynamic curves obtained on graphite and stainless steels in phosphoric acid (40% H_3PO_4) at 20 °C.

The graphite presented a good resistance in the acid medium; the current densities observed on this material were weak (less than 10^{-7} A/cm^2) until the potential value of 0.5 V/sce. When the anodic potential increased, the current density of graphite increased too, that was attributed to the formation of graphite oxide. It can be considered that the electrochemical corrosion of carbon in phosphoric acid proceeded through the formation of carbon surface oxides in preferred sites [34]. These sites are the edges, dislocations and discontinuities in the layer planes of microcrystalline carbon. At higher anodic potential values, the current increased rapidly with potential and then the anodic oxidation was the sum of many processes: oxidation of graphite electrode, decomposition of graphite oxide to CO_2 and CO and evolution of oxygen.

For stainless steels, it was clearly seen from Fig. 1 that the alloys had a good passive behaviour with a large passivation domain. This behaviour may be attributed to the chemical composition of the alloy rich on Cr, Ni and Mo. At anodic potentials, the formation of Fe, Cr and Ni oxides was expected following the reactions:

$$Fe + H_2O \rightarrow FeO + 2H^+ + 2e^-$$

$$Ni + H_2O \rightarrow NiO + 2H^+ + 2e^-$$

$$Cr + H_2O \rightarrow CrO + 2H^+ + 2e^-$$

The formation of iron oxide took place through a dissolution–precipitation mechanism in which the formed compound was soluble and started to deposit on the electrode surface, whereas the formation of both chromium and nickel oxides took place by direct nucleation and growth mechanism on the electrode surface. Then, the formation of higher oxidized forms of iron and chromium was expected as well as some thickening of nickel oxide:

$$2FeO + H_2O \rightarrow Fe_2O_3 + 2H^+ + 2e^-$$

$$2CrO + H_2O \rightarrow Cr_2O_3 + 2H^+ + 2e^-$$

Some authors considered that chromium oxide (Cr_2O_3) was the main passive component of the passive step in the anodic polarisation of SS [35]. Nickel was also able to reduce the corrosion rate and passive current density, and molybdenum addition in stainless steels was known to increase the resistance to localized and pitting corrosion [36]. The role of Ni and Mo in stainless steel at anodic potentials in acid solutions was to stabilise the passive film and to eliminate the active surface sites.

In the medium with high concentrations of phosphoric acid, precipitation of ironphosphate occurred at the interface [37]:

$$6H_3PO_4 + 3Fe \rightarrow 3Fe(H_2PO_4)_2 + 3H_2$$

$$3Fe(H_2PO_4)_2 \rightarrow Fe_3(PO_4)_2 + 4H_3PO_4$$

In these solutions and due to the low oxidative capacity of the stainless steel surface, a porous film formation was expected [38].

For the three stainless steels, the corrosion rate was about 4×10^{-7} A/cm^2 for HG, 8×10^{-7} A/cm^2 for UB64, 4×10^{-6} A/cm^2 for U50 and less than 2.5×10^{-8} A/cm^2 for graphite in the same conditions. These values indicated that all the tested materials were very resistant in the phosphoric acid solution with the best behaviour for graphite, then HG (high Ni and Mo contents), UB64 and U50 (lowest Ni and Mo contents).

3.2. *Influence of impurities*

Free potentials at open-circuit were recorded versus immersion time for graphite and stainless steels in the acid solution polluted with chloride and sulphate ions at 20 °C (Fig. 2). The evolution of the curves showed that all the samples may attain a steady-state open-circuit potential after a few minutes of immersion, indicating a good stability of the material/solution system even in the presence of impurities.

Potential values at open-circuit were 0.37, −0.07, −0.11 and −0.30 V/sce for Gr, HG, UB64 and U50, respectively. It can be seen that under the same conditions, the graphite showed a greater value of corrosion potential (more noble) than those

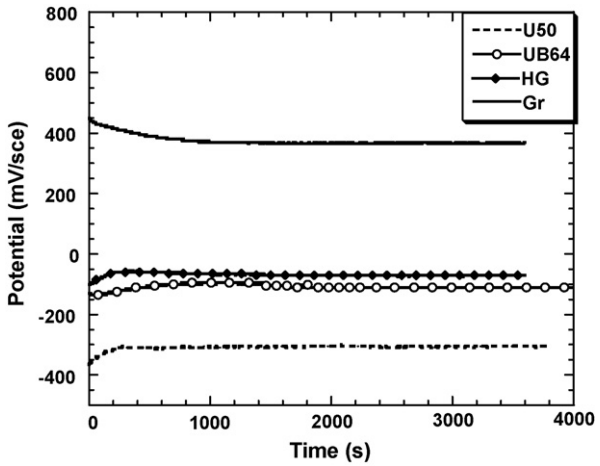

Fig. 2. Free potential vs. immersion time in polluted H_3PO_4 at 20 °C.

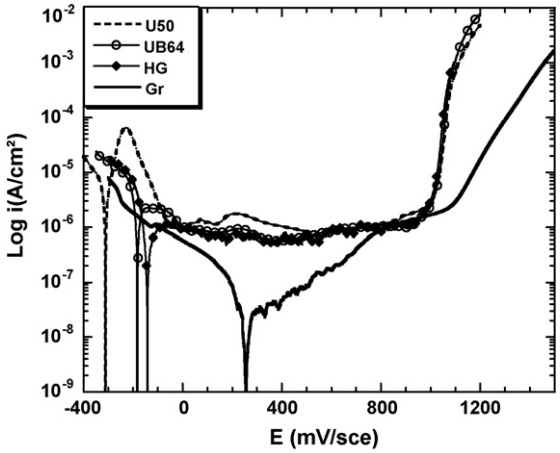

Fig. 3. Potentiodynamic curves obtained on graphite and stainless steels in polluted H_3PO_4 at 20 °C.

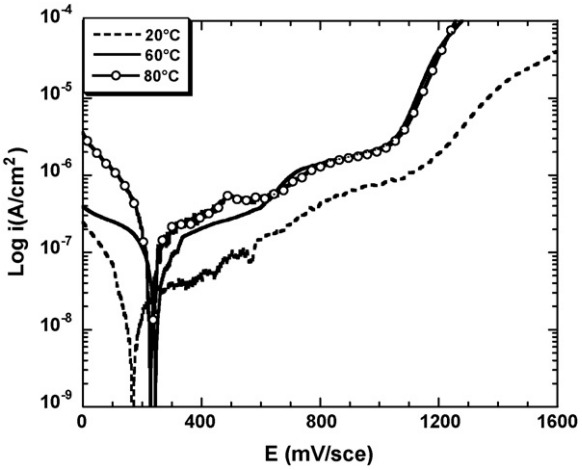

Fig. 4. Potentiodynamic curves obtained on graphite in H_3PO_4 at 20, 60 and 80 °C.

of stainless steels. This is due to the greater stability of the graphite surface in contact with polluted acid solution. Also, it may be assumed that at a free potential, the formation of a stable and protective layer was instantaneous on the stainless steel surfaces.

In the polluted acid with chloride and sulphate ions (Fig. 3), current densities on graphite and stainless steels were higher than those reported in Fig. 1. The presence of aggressive ions activated the material surfaces and then accelerated the corrosion rate. The corrosion current value was 2.5 times higher than in acid solution without impurities (10^{-6} A/cm^2 for the HG, 2×10^{-6} A/cm^2 for the UB64 and 10^{-5} A/cm^2 for U50). Comparing to graphite corrosion rate (4×10^{-8} A/cm^2) it can be concluded that stainless steels were more sensitive to the polluted acid attack than graphite.

For stainless steels, it was shown that the presence of impurities increased the anodic process. This effect was attributed to adsorption of aggressive ions on the material surface that prevented passivity [39] and accelerated local anodic dissolution. The growth of corrosion zones occurred as a result of an increase in aggressive ion concentration resulting from their migration inside the passive film [15,16].

In concentrated chloride solutions the presence of sulphate ions in the solution strongly increased the graphite anodic corrosion, but it was not noticed in dilute solutions [23]. The corrosion of graphite composite has been investigated by Beck et al. [24] in 1–18 M H_2SO_4 and 1–12 M $HClO_4$. The anodic reaction occurring in this process was the slow oxidation of graphite surface to C–COOH, CO and CO_2. Kokhanov [25] and Krishtalik and co-workers [26] studied the kinetic aspects of these reactions. Their investigations were carried out mostly in phosphate electrolytes where intercalation effects were small and the water (or hydroxyl ion) oxidation reaction predominated. The main product obtained under the anodic polarization was CO_2 in acid solution changing to oxygen in alkaline solution. This review showed that graphite was practically inert in alkaline or neutral solution, however in acidic solution electrochemically corrosion of graphite was observed with CO_2 evolution.

3.3. *Influence of temperature on graphite corrosion*

Polarization curves of graphite in phosphoric acid solution at 20, 60 and 80 °C are illustrated in Fig. 4. It can be seen that the increase of medium temperature induced an increase in current densities. Corrosion rate is about 2.5×10^{-8} A/cm^2 at 20 °C and more than 10^{-7} A/cm^2 at 80 °C.

The current values were bigger in polluted acid solution when the temperature of the medium increased (Fig. 5). From the data obtained, it was clearly seen that the stability of graphite was seriously disturbed by the increase of temperature up to 80 °C. The corrosion rate increased from 4×10^{-8} A/cm^2 at 20 °C to 4×10^{-7} A/cm^2 at 80 °C and the corrosion potential increased to more positive value (0.52 V/sce).

The increase of medium temperature induced an increase in the activity of the aggressive ions adsorbed on the surface, and consequently accelerated the dissolution process and the kinetic of exchange between the electrode surface and the electrolyte.

Temperature effect can be attributed to the appearance of active pores or defects in the graphite surface or to the diffusion of reagent species in the graphite layers. Kinoshita and Bett [20]

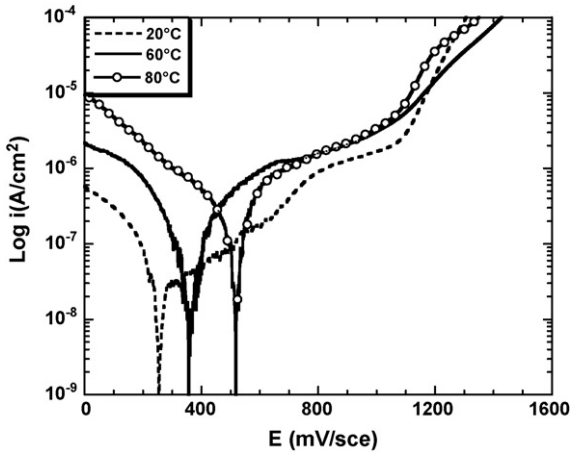

Fig. 5. Potentiodynamic curves obtained on graphite in polluted H_3PO_4 at 20, 60 and 80 °C.

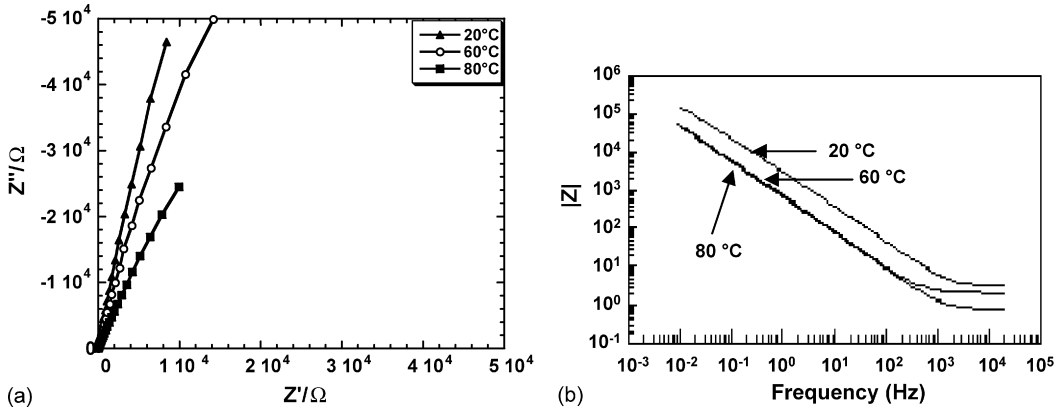

Fig. 6. Impedance spectroscopy curves for graphite in polluted H_3PO_4 at different temperatures: (a) Nyquist plots; (b) Bode plots.

investigated the electrochemical oxidation of different carbons in H_3PO_4 at temperature up to 130 °C. It was reported that two anodic processes occurred: the formation of a surface oxide and evolution of CO_2. Stonehart evaluated the effects of the electrolyte temperature and concentration, the operating potential, the type of carbon, and the nature of surface treatment on the specific carbon corrosion rates [40]. He found that at a given temperature the corrosion currents increased with higher potentials and at a given potential, the corrosion currents also increased with the temperature.

In order to confirm the electrochemical behaviour of graphite, impedance spectra were plotted at open-circuit potential in the polluted phosphoric acid at different temperatures. At high frequencies, linear curves were obtained in the Nyquist plots (Fig. 6a); these lines were not vertical, which indicated that the equivalent circuit of the system included a resistance in addition to the capacitive component [41]. The inclination of the lines was due to the presence of the finite faradaic resistance R_f in the equivalent circuit. This resistance is relatively large in the acid solution, because of the little rate of the graphite/electrolyte exchange at the steady-state potential.

Fig. 6b shows that there was a decrease in the total impedance values when the temperature of the electrolyte increased, revealing an increase of the corrosion rate. Indeed, the total impedance at 10^{-2} Hz was initially around $15 \times 10^4\ \Omega\,cm^2$ at 20 °C and decreased to value above $4 \times 10^4\ \Omega\,cm^2$ after increasing temperature to 80 °C. This evolution suggested an evolution of the charge exchange between the material and the solution occurring at the surface. The R_f value decreased when the temperature of acid medium increased (inclination of the plot was more pronounced) due to the enhanced rate of charge transfer at the interface. This evolution revealed that the corrosion processes became more important.

3.4. Local analysis

The scanning vibrating electrode technique was used to map the current distribution on the four materials after immersion in acid solutions. The main objective was to locate the cathodic and anodic regions, to compare corrosion resistance of the materials and then to obtain more information on the corrosion type attack which occurred on the materials surface in polluted phosphoric acid.

SVET scans are presented in Fig. 7. It was observed from the current maps that stainless steel and graphite surfaces reacted differently. After 60 min of immersion, the anodic and cathodic sites were distributed on the surface with different sizes and intensities. The sites of the metal dissolution or the formation of the surface oxides were indicated by the anodic zones (positive Iz), which were adjacent to the sites where the oxygen reduction occurred indicated by the cathodic zones (negative Iz).

Stainless steel surface showed big corrosion attack zones indicating a metallic corrosion activity with an anodic current density which attained 120 $\mu A/cm^2$ after immersion at free potential in the solution at room temperature (Fig. 7: map A–C). In the corrosive environments containing aggressive anions, passivity of alloys brook down at local points on the surface. At these points, anodic dissolution proceeded whereas the major part of surface remained passive.

Graphite samples showed a quasi-symmetric current distribution between anodic and cathodic sites, with size not exceeded a few tens of μms (Fig. 7: map D). The different sites were arbitrarily dispersed on the graphite surface and illustrated a uniform corrosion with weak current densities (less than 20 $\mu A/cm^2$).

When the samples of stainless steels were immersed in the acid solution at higher temperature (80 °C), bigger current densities were recorded and anodic sites were broader. The anodic activity of the stainless steels gave current density of at the most 120 $\mu A/cm^2$ at 20 °C and which exceeded 300 $\mu A/cm^2$ at 80 °C (Fig. 7: map E–G). The increase of temperature was confirmed to accelerate the dissolution kinetic on the metal surface. On the other hand, graphite surface was less affected by the increase of temperature: the current densities remained always moderate, but were also higher than those recorded at 20 °C (Fig. 7: map H). This was due to the increase of exchange rate in the active sites on the graphite surface and consequently the resistance of material decreased.

From all these results, current values recorded by SVET confirmed that graphite had the best resistance toward the acid aggressiveness than stainless steels in this order Gr > HG > UB64 > U50.

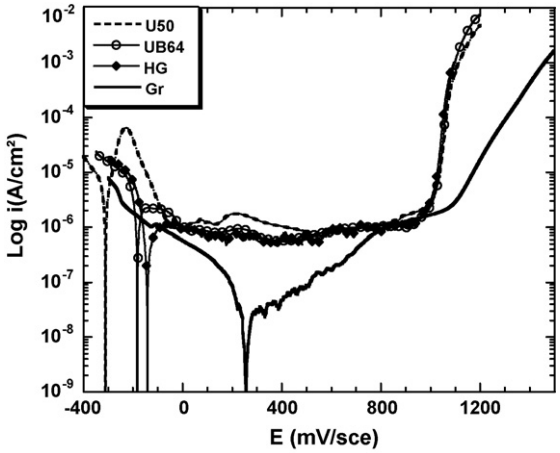

Fig. 3. Potentiodynamic curves obtained on graphite and stainless steels in polluted H_3PO_4 at 20 °C.

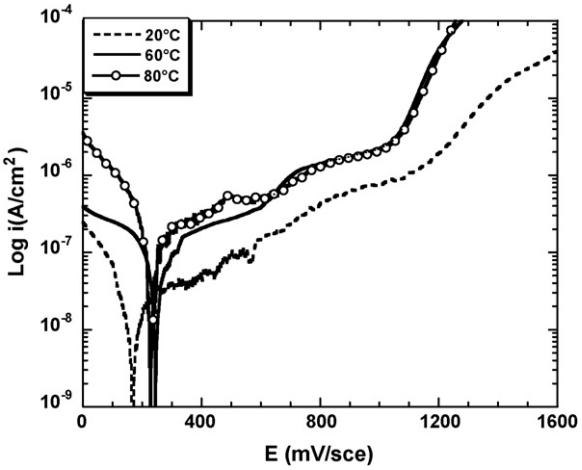

Fig. 4. Potentiodynamic curves obtained on graphite in H_3PO_4 at 20, 60 and 80 °C.

of stainless steels. This is due to the greater stability of the graphite surface in contact with polluted acid solution. Also, it may be assumed that at a free potential, the formation of a stable and protective layer was instantaneous on the stainless steel surfaces.

In the polluted acid with chloride and sulphate ions (Fig. 3), current densities on graphite and stainless steels were higher than those reported in Fig. 1. The presence of aggressive ions activated the material surfaces and then accelerated the corrosion rate. The corrosion current value was 2.5 times higher than in acid solution without impurities (10^{-6} A/cm^2 for the HG, 2×10^{-6} A/cm^2 for the UB64 and 10^{-5} A/cm^2 for U50). Comparing to graphite corrosion rate (4×10^{-8} A/cm^2) it can be concluded that stainless steels were more sensitive to the polluted acid attack than graphite.

For stainless steels, it was shown that the presence of impurities increased the anodic process. This effect was attributed to adsorption of aggressive ions on the material surface that prevented passivity [39] and accelerated local anodic dissolution. The growth of corrosion zones occurred as a result of an increase in aggressive ion concentration resulting from their migration inside the passive film [15,16].

In concentrated chloride solutions the presence of sulphate ions in the solution strongly increased the graphite anodic corrosion, but it was not noticed in dilute solutions [23]. The corrosion of graphite composite has been investigated by Beck et al. [24] in 1–18 M H_2SO_4 and 1–12 M $HClO_4$. The anodic reaction occurring in this process was the slow oxidation of graphite surface to C–COOH, CO and CO_2. Kokhanov [25] and Krishtalik and co-workers [26] studied the kinetic aspects of these reactions. Their investigations were carried out mostly in phosphate electrolytes where intercalation effects were small and the water (or hydroxyl ion) oxidation reaction predominated. The main product obtained under the anodic polarization was CO_2 in acid solution changing to oxygen in alkaline solution. This review showed that graphite was practically inert in alkaline or neutral solution, however in acidic solution electrochemically corrosion of graphite was observed with CO_2 evolution.

3.3. *Influence of temperature on graphite corrosion*

Polarization curves of graphite in phosphoric acid solution at 20, 60 and 80 °C are illustrated in Fig. 4. It can be seen that the increase of medium temperature induced an increase in current densities. Corrosion rate is about 2.5×10^{-8} A/cm^2 at 20 °C and more than 10^{-7} A/cm^2 at 80 °C.

The current values were bigger in polluted acid solution when the temperature of the medium increased (Fig. 5). From the data obtained, it was clearly seen that the stability of graphite was seriously disturbed by the increase of temperature up to 80 °C. The corrosion rate increased from 4×10^{-8} A/cm^2 at 20 °C to 4×10^{-7} A/cm^2 at 80 °C and the corrosion potential increased to more positive value (0.52 V/sce).

The increase of medium temperature induced an increase in the activity of the aggressive ions adsorbed on the surface, and consequently accelerated the dissolution process and the kinetic of exchange between the electrode surface and the electrolyte.

Temperature effect can be attributed to the appearance of active pores or defects in the graphite surface or to the diffusion of reagent species in the graphite layers. Kinoshita and Bett [20]

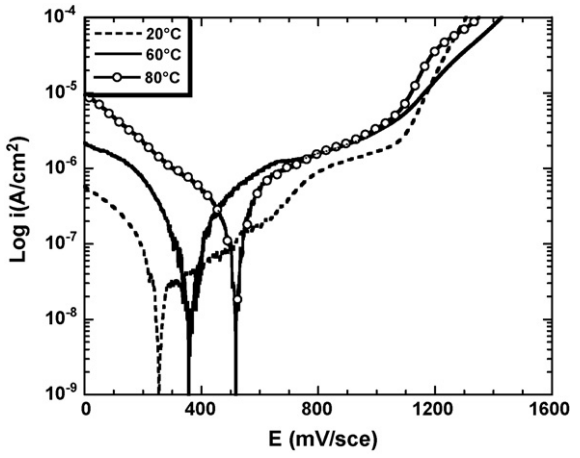

Fig. 5. Potentiodynamic curves obtained on graphite in polluted H_3PO_4 at 20, 60 and 80 °C.

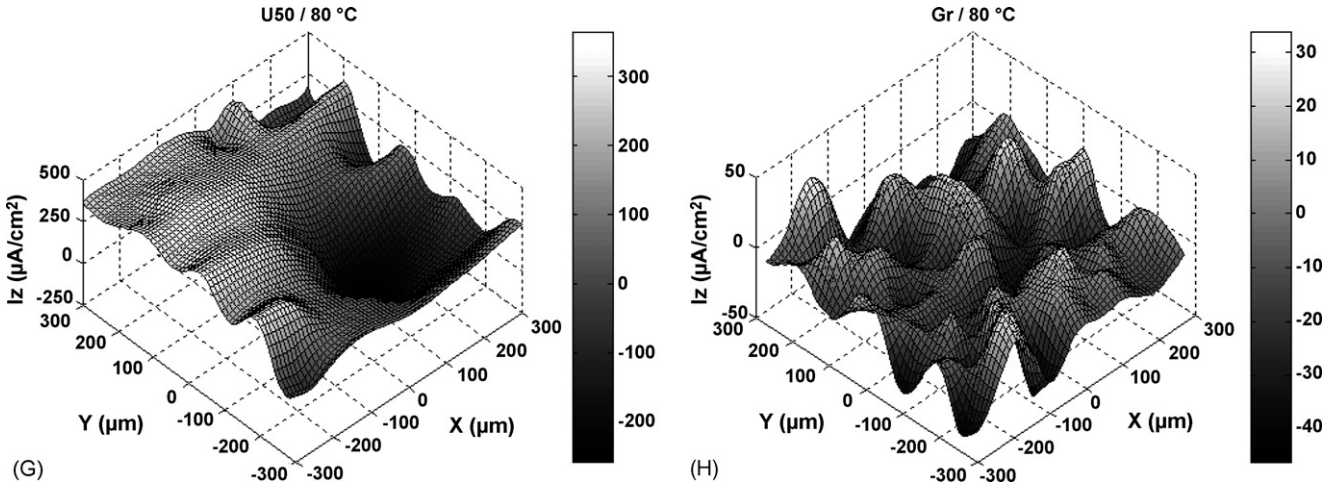

Fig. 7. (*Continued*).

4. Conclusions

The objectives of this study were to investigate the corrosion behaviour of graphite and stainless steels in phosphoric acid with and without chloride and sulphate ions at different temperatures. The addition of chemical impurities and the increase of the acid temperature, was used to mimic the industrial medium in order to understand the corrosion problems occurs during the phosphoric acid production.

In this paper, information were obtained with different electrochemical techniques. The classic techniques (polarization curves analysis, EIS) permitted to study the corrosion behaviour and to compare the resistance of the materials tested in the acid solution.

Therefore, combining the SVET to the traditional electrochemical techniques for local analysis made possible to study the corrosion process locally, and also to provide data from the corrosion type attack which occurred in the material surface in aggressive environment.

From this study, the following conclusions were:

- Compared to stainless steels, graphite material was more resistant with a low corrosion rate whatever the experimental condition (temperature and pollution).
- The presence of impurities as chloride and sulphate ions accentuated the aggressiveness of phosphoric acid.
- The increase of temperature induced an increase of the corrosion rate and an increase of the corrosion potential of tested materials.
- Impedance measurements showed that graphite had a good resistance in the phosphoric solution in agreement with polarisation curves results and the negative effect of medium temperature was also proved.
- The SVET analysis indicated that the corrosion which occurred on graphite was generalised corrosion whereas for stainless steel it was localized corrosion which made graphite an interesting component to be used in industrial process.

Acknowledgements

The authors acknowledge financial support of the Agence Universitaire de la Francophonie (AUF) and the Centre d'Etudes et de Recherches des Phosphates Minéraux, Morocco (CERPHOS) for alloys and graphite samples.

References

[1] P. Decker, Phosphates and Phosphoric Acid, Marcel Dekker Inc., New York, 1989.
[2] A. Guenbour, S. Zeggaf, A. Ben Bachir, M.L. Escudero, M.F. Lopez, Corrosion 55 (1999) 6.
[3] S. El hajjaji, L. Aries, N. Pebere, F. Dabosi, J.P. Audouard, A. Ben Bachir, Corros. Sci. 52 (1996) 11.
[4] A. Bellaouchou, A. Geunbour, A. Benbachir, Bull. Electrochem. 16 (2000) 166.
[5] A. Bellaouchou, A. Guenbour, A. Benbachir, Corrosion 49 (1993) 49.
[6] A. Guenbour, J. Faucheu, A. Ben Bachir, F. Dabosi, N. Bui, Br. Corros. J. 23 (4) (1988).
[7] A. Guenbour, H. Iken, N. Kebkab, A. Bellaouchou, R. Boulif, A. BenBachir, Appl. Surf. Sci. 252 (2006) 8710.
[8] H. Streblow, P. Marcus, Corrosion Mechanisms in Theory and Practice, Marcel Dekker, New York, 1995.
[9] S. Rajeswari, K.S.K. Danadurai, T.M. Sridhar, S.V. Narasimhan, Corrosion 57 (2001) 465.
[10] J.H. Qiu, Surf. Interface Anal. 33 (2002) 830.
[11] G.C. Frenkel, J. Electrochem. Soc. 145 (1998) 2186.
[12] M.A. Ameer, A.M. Fekry, F. El-Taib Heakal, Electrochim. Acta 50 (2004) 43.
[13] A. Galal, N.F. Atta, M.H.S. Al-Hassan, Mater. Chem. Phys. 89 (2005) 38.
[14] S.A.M. Refaey, F. Taha, A.M. Abd El-Malak, Appl. Surf. Sci. 242 (2005) 114.
[15] S.A.M. Refaey, Appl. Surf. Sci. 157 (2000) 199.
[16] S.S. Abd El Rehim, S.A.M. Refaey, F. Taha, M.B. Saleh, R.A. Ahmed, J. Appl. Electrochem. 31 (2001) 435.
[17] O. Yamamoto, K. Imai, T. Sasamoto, J. Eur. Ceram. Soc. 12 (1993) 4.
[18] T.L. Dhami, O.P. Bahl, B.R. Awasthy, Carbon 33 (1995) 7.
[19] K. Kinoshita, Carbon Electrochemical and Physicochemical Properties, Wiley, New York, 1987.
[20] K. Kinoshita, J.A.S. Bett, Carbon 11 (1973) 237.
[21] K. Kinoshita, J.A.S. Bett, in: C. Tedmon Jr. (Ed.), Corrosion Problems in Energy Conversion and Generation, Electochim. Soc., Princeton, New Jersey, 1974.

[22] L.J. Janssen, J.G. Hoogland, Electrochim. Acta 15 (1970) 339.
[23] F. Hine, M. Yassuda, I. Sugiara, T. Nuda, J. Electrochem. Soc. 121 (1974) 220.
[24] F. Beck, H. Krohn, E. Zimmer, Electrochim. Acta 31 (1986) 371.
[25] G.N. Kokhanov, Elektrokhemya 7 (1971) 1606.
[26] N.T. Piet, D.V. Kokoulina, L. Krishtalik, Elektrokhemya 8 (1972) 384.
[27] J. Jiang, F. Beck, Carbon 30 (1992) 2.
[28] A. Metrot, H. Fuzellier, Carbon 22 (1984) 2.
[29] B. Vuillemin, X. Philippe, R. Oltra, V. Vignal, L. Coudreuse, L.C. Dufour, E. Finot, Corros. Sci. 45 (2003) 1143.
[30] H. Uchida, M. Yamashita, S. Inoue, K. Koterazawa, Mater. Sci. Eng. A 319–321 (2001) 496.
[31] I. Sekine, M. Yuasa, N. Hirose, T. Tanaki, Prog. Org. Coat. 45 (2002) 1.
[32] M. Khobaib, A. Rensi, T. Matakis, M.S. Donley, Prog. Org. Coat. 41 (2001) 266.
[33] H. Krawiec, V. Vignal, R. Oltra, Electrochem. Commun. 6 (2004) 655.
[34] P. Stonehart, Prog. Batteries Solar Cells 5 (1984) 260.
[35] M. Abdellah, Mater. Chem. Phys. 82 (2003) 786.
[36] L. Wegrelius, F. Fakenberg, I. Olefjord, J. Electrochem. Soc. 146 (1999) 3.
[37] E. Almeida, D. Pereira, M.O. Figueiredo, V.M.M. Lobo, M. Morcillo, Corros. Sci. 39 (1997) 1561.
[38] S.R. Moraes, D. Huerta-Vilca, A.J. Motheo, Prog. Org. Coat. 48 (2003) 28.
[39] P. Marcus, J. Chem. Phys. 88 (1991) 1697.
[40] P. Stonehart, Carbon 22 (1984) 4.
[41] J.R. Macdonald, W.B. Johnson, in: J.R. Macdonald (Ed.), Impedance Spectroscopy, Wiley, New York, 1987, p. 112.